ISSN 0021-3640, JETP Letters, 2014, Vol. 99, No. 2, pp. 67–75. © Pleiades Publishing, Ltd., 2014.
Original Russian Text © N.V. Volkov, I.A. Gudim, E.V. Eremin, A.I. Begunov, A.A. Demidov, K.N. Boldyrev, 2014, published in Pis'ma v Zhurnal Eksperimental'noi i Teoreticheskoi Fiziki, 2014, Vol. 99, No. 2, pp. 72–80.

Magnetization, Magnetoelectric Polarization, and Specific Heat of $HoGa_3(BO_3)_4$

N. V. Volkov[a], I. A. Gudim[a], E. V. Eremin[a], A. I. Begunov[b], A. A. Demidov[b, *], and K. N. Boldyrev[c]

[a] *Kirensky Institute of Physics, Siberian Branch, Russian Academy of Sciences, Akademgorodok, Krasnoyarsk, 660036 Russia*

[b] *Bryansk State Technical University, Bryansk, 241035 Russia*

* *e-mail: demandr@yandex.ru*

[c] *Institute of Spectroscopy, Russian Academy of Sciences, Troitsk, Moscow region, 142190 Russia*

Received November 8, 2013

A comprehensive experimental and theoretical study of magnetic, magnetoelectric, thermal, and spectroscopic characteristics of $HoGa_3(BO_3)_4$ gallium borate single crystals has been performed. A large magnetoelectric effect exceeding its values found in all iron and aluminum borates except $HoAl_3(BO_3)_4$ has been observed. The magnetoelectric polarization of $HoGa_3(BO_3)_4$ equals $\Delta P_{ba}(B_a) \approx -1020$ μC/m^2 at $T = 5$ K in a magnetic field of 9 T. The theoretical treatment based on the crystal field model for rare-earth ions provides a unified approach for the consistent interpretation of all measured characteristics. The crystal-field parameters are determined. The temperature (in the 3–300 K range) and magnetic field (up to 9 T) dependences of the magnetization, the Schottky anomaly in the temperature dependence of the specific heat, and its shift in the field **B** || **c** are described. To compare the thermal properties of $HoGa_3(BO_3)_4$ with those of $HoAl_3(BO_3)_4$ exhibiting record values of the polarization, the specific heat of $HoAl_3(BO_3)_4$ at various B values and the temperature dependence of the polarization $\Delta P_b(T)$ in the applied magnetic field of 9 T have been measured.

DOI: 10.1134/S0021364014020106

INTRODUCTION

Rare-earth borates $RM_3(BO_3)_4$ (where R = Y, La–Lu; M = Fe, Al, Cr) actively studied now have a trigonal crystal structure and multiferroic properties important for applications (see, e.g., [1–7] and review [8]). The borates with two magnetic subsystems ($RFe_3(BO_3)_4$ iron borates) appear to be multiferroics with the coexisting magnetic, electric, and elastic order parameters [1–3, 5–8]. The quantum theory of magnetoelectricity has been recently formulated for such compounds [9]. The borates with a single magnetic subsystem ($RAl_3(BO_3)_4$ aluminum borates) exhibit a combination of good luminescent and clearly pronounced nonlinear optical properties as well as recently discovered strong multiferroicity [10–12].

The growing interest in $RM_3(BO_3)_4$ borates is stimulated by the discovery of the giant magnetoelectric effect in $HoAl_3(BO_3)_4$. In $HoAl_3(BO_3)_4$, the record value of the magnetoelectric polarization is as large as $\Delta P_{ba}(B_a) \approx -3600$ μC/m$_2$ at $T = 3$ K in a magnetic field of 7 T [11]. This value is several times higher than all known maximum values of the polarization, including those in iron borates. In [13], it is reported that the polarization in $HoAl_3(BO_3)_4$ achieves the value $\Delta P_{ba}(B_a) \approx -5240$ μC/m^2 at $T = 5$ K in a magnetic field of 9 T, which far exceeds the previous record described in [11].

In $RM_3(BO_3)_4$, the replacement of the magnetic system (Fe) by the nonmagnetic one (Al) leads to a giant magnitude of the magnetoelectric effect. Therefore, it is of interest to study other subclasses of borates with only one magnetic subsystem, in particular, that with holmium ions, $HoM_3(BO_3)_4$. This provides an opportunity to compare their characteristics with the records achieved in $HoAl_3(BO_3)_4$.

The present work deals with experimental and theoretical studies of the magnetic, magnetoelectric, thermal, and spectroscopic characteristics of a typical representative of a novel subclass of borates, namely, $HoGa_3(BO_3)_4$ gallium borate, and their comparison to the properties of $HoAl_3(BO_3)_4$.

EXPERIMENT

$HoGa_3(BO_3)_4$ single crystals were grown using the solution-melts based on bismuth trimolybdate and lithium molybdate [14] (68 wt % [$Bi_2Mo_3O_{12}$ + 2Bi_2O_3 + 0.3Ho_2O_3] + 32 wt % $HoGa_3(BO_3)_4$) according to the technology described in detail in [15]. The grown crystals 5–8 mm in size have a small pinacoidal {0001} face perpendicular to the C_3 axis. The magnetic character-

istics and the specific heat have been measured by a Quantum Design PPMS-9 physical property measurement system within the 2–300 K temperature range at the applied magnetic field up to 9 T. The magnetoelectric effects were studied through the use of a Keithley 6517B electrometer by measuring the charge between two contacts (made of epoxy resin with a conducting filler) applied to the opposite sides of the plane-parallel plate. The absorption spectra were recorded within wide temperature (3.2–300 K) and spectral (2000–25 000 cm^{-1}) ranges by a Bruker IFS 125HR Fourier spectrometer with a spectral resolution of 0.1 cm^{-1}. To obtain the data on the sequence of energy levels in the ground state, we measured the absorption spectra for the linearly polarized light in the geometry corresponding to $\mathbf{k} \perp c$, $\mathbf{E} \perp c$ (σ polarization) and $\mathbf{k} \perp c$, $\mathbf{E} \perp c$ (π polarization).

CALCULATION TECHNIQUE

In the calculations, we use our experience and the results accumulated in the successful studies of the compounds isostructural to $HoGa_3(BO_3)_4$ gallium borate, such as $HoAl_3(BO_3)_4$ [13, 16, 17], $HoFe_3(BO_3)_4$ iron borate [18, 19] (as well as iron borates with other elements R, see, e.g., [3, 20]), paramagnetic zircons RXO_4 (X = P, V) (see, e.g., [21]), and $HoBa_2Cu_3O_{7-x}$ [22].

To calculate the magnetic characteristics and the Zeeman effect, we use Hamiltonian $\mathcal{H}$, including the crystal-field (CF) Hamiltonian $\mathcal{H}_{CF}$, the Zeeman term $\mathcal{H}_Z$, and the Hamiltonian $\mathcal{H}_{HF}$ describing the hyperfine interaction

$$\mathcal{H} = \mathcal{H}_{CF} + \mathcal{H}_Z + \mathcal{H}_{HF}, \quad (1)$$

$$\mathcal{H}_{CF} = B_0^2 C_0^2 + B_0^4 C_0^4 + B_3^4 (C_{-3}^4 - C_3^4) + B_0^6 C_0^6 + B_3^6 (C_{-3}^6 - C_3^6) + B_6^6 (C_{-6}^6 + C_6^6), \quad (2)$$

$$\mathcal{H}_Z = -g_J \mu_B \mathbf{B}\mathbf{J}, \quad (3)$$

$$\mathcal{H}_{HF} = A_J \mathbf{J}\mathbf{I}. \quad (4)$$

In these expressions, B_q^k are the crystal field parameters for the D_3-symmetry, C_q^k are the irreducible tensor operators, g_J is the Landé g-factor, $\mathbf{J}$ is the angular momentum operator for the R ion, A_J is the hyperfine coupling constant ($A_J \approx 0.027$ cm^{-1} [23]), and $\mathbf{I}$ is the nuclear spin operator.

The magnetization of paramagnetic $HoGa_3(BO_3)_4$ in the applied magnetic field $\mathbf{B}$ is

$$\mathbf{M} = g_J \mu_B \langle \mathbf{J} \rangle. \quad (5)$$

The contribution of the Ho subsystem to the specific heat of $HoGa_3(BO_3)_4$ is calculated according the formula

$$C_{Ho} = k_B \frac{\langle E^2 \rangle - \langle E \rangle^2}{(k_B T)^2}. \quad (6)$$

The thermal averages $\langle E^2 \rangle$ and $\langle E \rangle^2$ are calculated on the spectrum of the Ho^{3+} ion formed by the crystal field and the applied magnetic field.

RESULTS AND DISCUSSION

The description of the magnetic properties of $HoGa_3(BO_3)_4$ should be started from finding out the CF parameters B_q^k, since it is just CF which forms the electron structure of a rare-earth ion (its spectrum and wavefunctions) and is responsible for the anisotropy of magnetic properties. Note that data on the physical properties of gallium borates are almost absent (except the results of the crystal structure studies). This creates significant difficulties in determining the CF parameters for $HoGa_3(BO_3)_4$.

In [13], the CF parameters of the Ho^{3+} ion in the isostructural compound $HoAl_3(BO_3)_4$ are determined on the basis of the fitting of experimental data on the temperature and magnetic field dependences of the magnetization. Then, in [17], it is reported that a slight refinement (~1–6%) of the CF parameters found in [13] allows for a qualitative description of the behavior of the measured magnetostriction for $HoAl_3(BO_3)_4$ [11]. At the same time, this also provides a good description for the magnetic characteristics reported in [13]. As a result, the initial values of the CF parameters in $HoGa_3(BO_3)_4$, from which starts the minimization procedure for the corresponding objective function, are chosen similar to those for the isostructural compounds $HoAl_3(BO_3)_4$ [13, 17] and $YAl_3(BO_3)_4$:Ho^{3+} [24], as well as for $HoFe_3(BO_3)_4$ [18].

It is interesting that our spectroscopic studies demonstrate that the Stark structure of the energy levels in the ground-state multiplet of the Ho^{3+} ion in $HoGa_3(BO_3)_4$ differs to a certain extent from the corresponding structure in $HoAl_3(BO_3)_4$, which coincides with the earlier determined structure for $YAl_3(BO_3)_4$:Ho^{3+} [24]. At the same time, the differences between the corresponding energy levels in $HoGa_3(BO_3)_4$ and in $HoAl_3(BO_3)_4$ are quite close to each other. In $HoGa_3(BO_3)_4$, the analysis of the measured transmission spectra allows us to identify the following energy levels in the ground-state multiplet of the Ho^{3+} ion (here, superscript d denotes the doublet): 0^d, 10.7, 13.2^d, 30.1, 109, 120.7^d, 152.5, 181.1^d, 209.3^d, 246.2, and 267^d cm^{-1}. We can see that the lower part of the multiplet includes the doublet–singlet–doublet

sequence rather than the doublet–doublet–singlet sequence characteristic of $HoAl_3(BO_3)_4$ exhibiting the record polarization values (see [24]).

To determine the CF parameters, in the objective function, we specify the information about the certain structure of the ground-state multiplet (the sequence of singlets and doublets, energy values), as well as the data on the magnetization curves $M_{c,\perp c}(B)$ at $T = 3$ K in the applied magnetic field up to 9 T and on the temperature dependence of the magnetization $M_{c,\perp c}(T)$ in the 3–300 K range at $B = 0.1$ and 6 T. As a result, following the criteria for the description of $M_{c,\perp c}(B)$ and $M_{c,\perp c}(T)$ and for reproducing the structure of the ground-state multiplet, we chose the set of parameters providing the most adequate description of the whole block of experimental data (B_q^k are given in units of cm^{-1})

$$B_0^2 = 125, \quad B_0^4 = -1740, \quad B_3^4 = -206,$$
$$B_0^6 = 65, \quad B_3^6 = -323, \quad B_6^6 = 269. \qquad (7)$$

In the calculations, these parameters are determined using the basis corresponding to the ground-state multiplet. Therefore, they can be treated only as the effective values applicable for the description of the thermodynamics of $HoGa_3(BO_3)_4$.

Parameter set (7) corresponds to the following energy values for the 17 lowest Stark levels of the ground-state multiplet of the Ho^{3+} ion in $HoGa_3(BO_3)_4$ ($B = 0$, $T = 3$ K): 0^d, 9.9, 12.4^d, 31, 97, 150^d, 202, 234^d, 275^d, 298, and 311^d cm^{-1}. The structure of the energy levels in the ground-state multiplet obtained in the calculations exactly reproduces that determined in the experiment. The calculated energy values are close to the measured ones in the lower part of the multiplet, which is mainly responsible for the thermodynamic characteristics of $HoGa_3(BO_3)_4$ within the temperature range studied in the experiment.

In Fig. 1, we show the magnetization curves $M_{c,\perp c}(B)$ for $HoGa_3(BO_3)_4$ at $T = 3$ and 295 K. At $T = 3$ K, we can see that the components of magnetization grow with the magnetic field at different rates, thus exhibiting a clearly pronounced anisotropy. The magnetization curves calculated using parameters (7) agree well with the corresponding experimental curves at both $T = 3$ and 295 K. The comparison of $M_{c,\perp c}(B)$ plots for $HoGa_3(BO_3)_4$ and $HoAl_3(BO_3)_4$ (see Fig. 1 in [13]) shows that the replacement of Al^{3+} by Ga^{3+} leads to a slight decrease in the anisotropy. At the same time, $M_c(B)$ increases quite slowly with the magnetic field (by about 3%), whereas $M_{\perp c}(B)$ grows much faster. This leads to a decrease in the field value at which these components become equal by 2.2 T. The magnitude of the Zeeman effect corresponding to the calculated $M_{c,\perp c}(B)$ plots at $T = 3$ K is illustrated in the inset

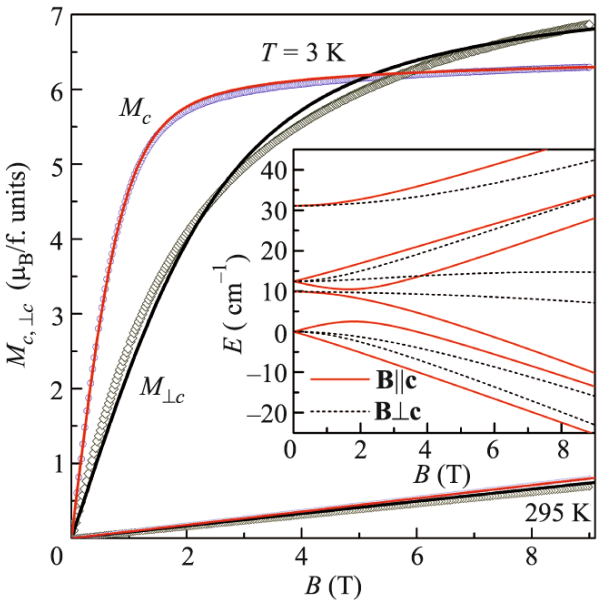

Fig. 1. (Color online) Magnetization curves of $HoGa_3(BO_3)_4$ for $\mathbf{B} \parallel \mathbf{c}$ and $\mathbf{B} \perp \mathbf{c}$ at $T = 3$ and 295 K. Symbols denote the experimental data and the lines correspond to the calculations. The inset illustrating the Zeeman effect at $T = 3$ K shows the six lowest levels of the ground-state multiplet for Ho^{3+} ion at (solid lines) $\mathbf{B} \parallel \mathbf{c}$ and (dashed lines) $\mathbf{B} \perp \mathbf{c}$.

of Fig. 1. The splitting of the energy levels of Ho^{3+} ions, being larger at $\mathbf{B} \parallel \mathbf{c}$ than at $\mathbf{B} \perp \mathbf{c}$, determines the observed behavior of $M_{c,\perp c}(B)$ plots. The faster increase in $M_{\perp c}(B)$ with the field for $HoGa_3(BO_3)_4$ than that for $HoAl_3(BO_3)_4$ is related to a larger splitting of the lower levels at $\mathbf{B} \perp \mathbf{c}$ (see inset of Fig. 1 in [13]).

In Fig. 2, we show the temperature dependence of the magnetization $M_{c,\perp c}(T)$ at $B = 0.1$ T. We see that the calculated curves agree rather well with the experimental ones. Here, similar to $HoAl_3(BO_3)_4$, the $M_{\perp c}(T)$ curve calculated at the lowest temperatures tends to the constant value $M_{\perp c} = 0.24$ μ_B/formula unit (see inset of Fig. 2). Note that the characteristic features of the measurements performed at $\mathbf{B} \perp \mathbf{c}$ suggest that the misalignment of about 5°, which could be responsible for the difference in the description of $M_{\perp c}(T)$ observed at low T, is quite improbable.

For the compounds with Ho^{3+} ions, the effect of the hyperfine interaction on the magnetic characteristics becomes more significant at low temperatures and can eventually become dominant. Therefore, we calculate $M_{c,\perp c}(T)$ taking into account hyperfine interaction (4). Similar to the case of $HoAl_3(BO_3)_4$, the calculations demonstrate the possibility of a slight growth of $M_{\perp c}(T)$ only at $T < 1.7$ K (the green curve in the inset of Fig. 2). Thus, taking into account the hyperfine interaction in form (4) with $A_J \approx 0.027$ cm^{-1} [23] does not lead to significant improvements in the

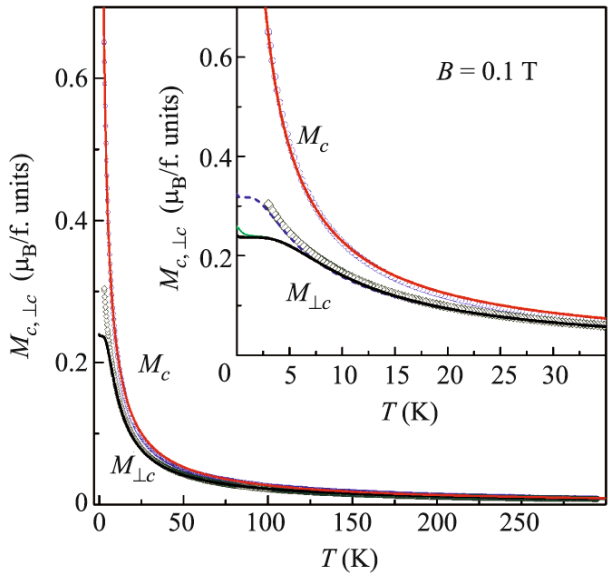

Fig. 2. (Color online) Temperature dependence of magnetization $M_{c,\perp c}(T)$ for $HoGa_3(BO_3)_4$ at $B = 0.1$ T. Symbols denote the experimental data and the lines correspond to the calculations. The inset demonstrates the low-temperature portion of the $M_{c,\perp c}(T)$ curves (the green line corresponds to the calculations taking into account the hyperfine interactions and the blue dashed line illustrates the calculations using the CF parameters giving $\Delta \sim 6$ cm^{-1}).

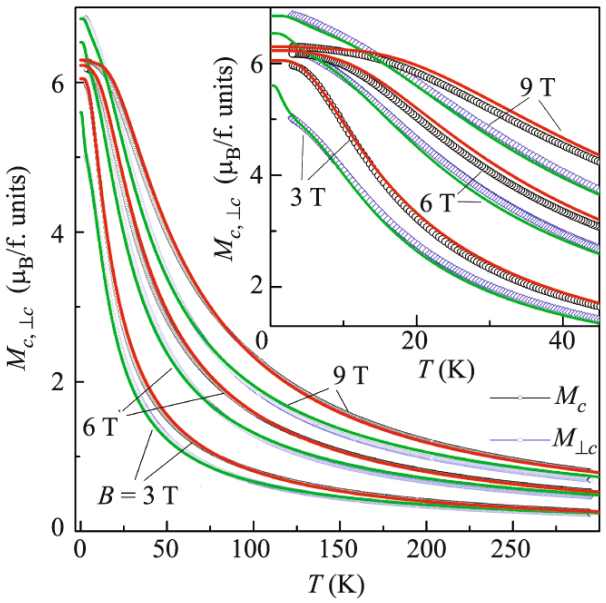

Fig. 3. (Color online) Temperature dependence of magnetization $M_{c,\perp c}(T)$ for $HoGa_3(BO_3)_4$ at $B = 3$, 6, and 9 T. Symbols denote the experimental data and the lines correspond to the calculations: red and green curves correspond to $M_c(T)$ and $M_{\perp c}(T)$, respectively. The inset demonstrates the low-temperature portion of the $M_{c,\perp c}(T)$ curves.

description of $M_{\perp c}(T)$ at the lowest temperatures. We also performed the calculations including the nuclear Zeeman coupling ($\mathcal{H}_Z = -\gamma_I \hbar \mathbf{BI}$). This means that we add the effective nuclear spin Hamiltonian describing the hyperfine interaction (see, e.g., [25]) to Hamiltonian (1). For $HoGa_3(BO_3)_4$, the parameters characterizing the spin Hamiltonian are unknown. Therefore, we perform the calculations using the parameters characteristic of $HoVO_4$ [25]. We find that the inclusion of the nuclear Zeeman coupling in the field $B =$ 0.1 T can lead to a better description of $M_{\perp c}(T)$ only if we increase parameter $\gamma_\perp/2\pi$ by a factor of 5 (for $HoVO_4$, we have $\gamma_\perp/2\pi = 1527$ MHz/T [25]). As a result, we conclude that the possible future determination of the parameters of the spin Hamiltonian for $HoGa_3(BO_3)_4$ should allow us to determine more accurately the degree of responsibility of the hyperfine interaction for the observed difference between the measured and theoretical $M_{\perp c}(T)$ curves at $T < 3$ K.

We have demonstrated that, varying the CF parameters, we can achieve a much better description of $M_{\perp c}(T)$. For this purpose, the splitting between the lowest levels should be $\Delta \sim 6$ cm^{-1} instead of 10.7 cm^{-1} determined from the experimental data. The $M_{\perp c}(T)$ curve calculated with the CF parameters giving $\Delta \sim$ 6 cm^{-1} accurately reproduces the experimental curve (dashed line in inset of Fig. 2) and tends to the constant value $M_{\perp c} = 0.32$ μ_B/formula unit. The description of $M_{\perp c}(B)$ also becomes better. However, $\Delta \sim$ 6 cm^{-1} gives rise to the Schottky anomaly near 3.5 K in the temperature dependence of the specific heat $C(T)$, whereas the experimental value is 7.8 K (see below). Taking into account these differences in the description of Δ_{exp} and the Schottky anomaly, we choose for the CF parameters values (7), which give a good description on average for all measured characteristics and are much nearer to the energy values measured in the experiment.

In Fig. 3, we show the $M_{c,\perp c}(T)$ plots at high values of the applied magnetic field ($B = 3$, 6, and 9 T). We can see that, at low temperatures (see inset of Fig. 3), the anisotropy of $M_{c,\perp c}(T)$ at different B values undergoes significant changes. At the same time, it is fitted well within the whole temperature range under study. The calculation corresponding to $T < 3$ K allows predicting the form of $M_{c,\perp c}(T)$ in the temperature range outside that studied in the experiment. The analysis of the $M_c/M_{\perp c}$ values demonstrates the decrease in the magnetic anisotropy in comparison to that observed for $HoAl_3(BO_3)_4$. At $T = 3$ K, we have (in brackets, we give the corresponding values for $HoAl_3(BO_3)_4$) $M_c/M_{\perp c} = 2.14$ (2.83), 1.16 (1.32), 0.98 (1.05), and 0.92 (0.98) at $B = 0.1$, 3, 6, and 9 T, respectively. At $T = 15$ K, we have $M_c/M_{\perp c} = 1.26$ (1.43), 1.19 (1.31), 1.07 (1.14), and 1 (1.04) at $B = 0.1$, 3, 6, and 9 T, respectively.

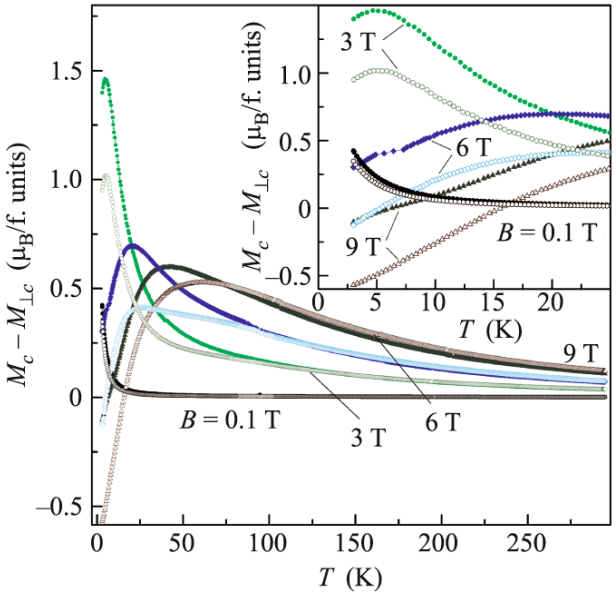

Fig. 4. (Color online) Experimental temperature dependence of $M_c - M_{\perp c}(T)$ for (open circles) $HoGa_3(BO_3)_4$ and (closed circles) $HoAl_3(BO_3)_4$ at $B = 0.1$, 3, 6, and 9 T. The inset demonstrates the low-temperature portion of the $M_c - M_{\perp c}(T)$ curves.

In Fig. 4, we show the experimental plots of $M_c - M_{\perp c}(T)$ for (open circles) $HoGa_3(BO_3)_4$ and (closed circles) $HoAl_3(BO_3)_4$ at $B = 0.1$, 3, 6, and 9 T. These curves help us to understand how the magnetic anisotropy depends on the temperature and magnetic field in the compounds under study. We see that the $M_c - M_{\perp c}(T)$ curves are located lower (lower anisotropy) for $HoGa_3(BO_3)_4$ than the corresponding curves for $HoAl_3(BO_3)_4$, except the high-temperature portions of these curves at $B = 6$ T (at $T > 120$ K) and at $B = 9$ T (at $T > 75$ K). For $HoGa_3(BO_3)_4$, the low-temperature range at $B = 9$ T, where $M_c < M_{\perp c}$, is slightly broader than that for $HoAl_3(BO_3)_4$. The range where $M_c < M_{\perp c}$ also appears at $B = 6$ T and this range is quite similar to that corresponding to 9 T for $HoAl_3(BO_3)_4$. As a result, at $T = 3$–6 K, the magnetic anisotropy appearing in $HoAl_3(BO_3)_4$ at 9 T coincides with that in $HoGa_3(BO_3)_4$ at 6 T. Hence, the aforementioned values of the magnetization ratio at $T = 3$ K also coincide, $(M_c/M_{\perp c})^{\mathrm{HoGa}}_{6\,\mathrm{T}} = (M_c/M_{\perp c})^{\mathrm{HoAl}}_{9\,\mathrm{T}}$.

Note also that, if we increase the temperature, for any value of B, there exists such a temperature value beginning from which the difference in anisotropy between $HoGa_3(BO_3)_4$ and $HoAl_3(BO_3)_4$ decreases appreciably and nearly vanishes at low values of B. With the growth of the magnetic field, such a characteristic temperature varies nonmonotonically: $T \approx 40$, 140, 120, and 75 K at $B = 0.1$, 3, 6, and 9 T, respectively.

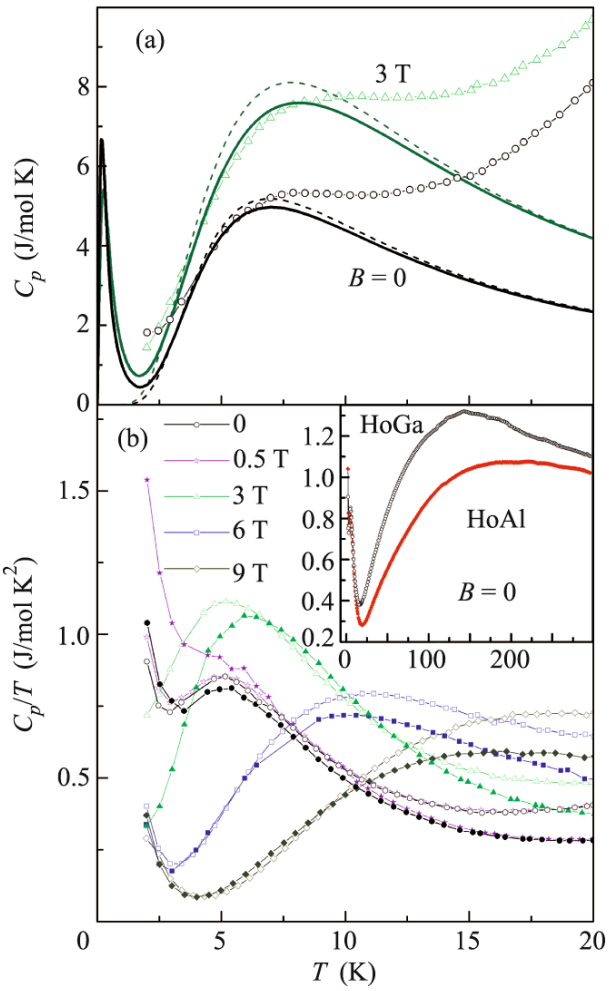

Fig. 5. (Color online) (a) Specific heat $C_p(T)$ of $HoGa_3(BO_3)_4$ at $B_c = 0$ and 3 T and $T = 2$–20 K and the contribution $C_{\mathrm{Ho}}(T)$ of the Ho subsystem to the total specific heat calculated (solid lines) with and (dashed lines) without the hyperfine interaction. (b) Specific heat $C_p/T(T)$ of (open symbols) $HoGa_3(BO_3)_4$ and (closed symbols) $HoAl_3(BO_3)_4$ at $B_c = 0$, 0.5, 3, 6, and 9 T.

The experimental data on the specific heat for $HoGa_3(BO_3)_4$ at $B = 0$ and in the magnetic field applied along the c axis are presented in Fig. 5a. The broad peaks in the $C_p(T)$ curves clearly seen near 7.8 K (at $B = 0$) and near 9 K (at $B_c = 3$ T) correspond to the Schottky anomalies. Using CF parameters (7) determined by the analysis of the magnetic characteristics and the splittings in the ground-state multiplet, we have calculated the contribution $C_{\mathrm{Ho}}(T)$ of the Ho subsystem to the total specific heat (solid lines) including and (dashed lines) excluding the hyperfine interaction (see Fig. 5a). We can see that the peaks in the dashed curves calculated without the hyperfine interaction agree well with the experimental curves. In agreement with the experiment, these peaks become displaced toward higher T values at $\mathbf{B} \parallel \mathbf{c}$. The calcula-

tions demonstrated that the observed Schottky anomaly is related to the redistribution in the populations of the two lowest doublets. Its position on the temperature axis is determined by the energy difference between these doublets. The inclusion of the hyperfine interaction in form (4) leads to the splitting of the levels (into eight components, $I = 7/2$ for ^{165}Ho). As a result, there appear additional sharp peaks (Schottky anomalies) in the $C_{\mathrm{Ho}}(T)$ curves near 0.2 K. This somehow improves the description of the broad peaks observed in the experiment.

The existence and positions of the Schottky anomalies are very sensitive to the specific values of the energy difference between the lowest levels. Therefore, it is interesting to compare the specific heat plots for $HoGa_3(BO_3)_4$ and $HoAl_3(BO_3)_4$. These plots for (open symbols) $HoGa_3(BO_3)_4$ and (closed symbols) $HoAl_3(BO_3)_4$ with $C_p/T(T)$ put on the vertical axis are shown in Fig. 5b for $B = 0$, 0.5, 3, 6, and 9 T and $T =$ 2–20 K (the plot for T up to 300 K at $B = 0$ is shown in the inset). We can see that the difference between the specific heat values for these compounds at $B = 0$, 0.5, and 3 T is observed both at low T and near 20 K. At high applied magnetic fields ($B = 6$ and 9 T), the difference becomes visible with the growth of temperature. This implies the difference in the behavior of the energy levels in the ground-state multiplets of the Ho^{3+} ion for $HoGa_3(BO_3)_4$ and $HoAl_3(BO_3)_4$ under the effect of the applied magnetic field and hence the difference in the magnetic contribution to the specific heat. It is mentioned above that the spectroscopic studies allow us to find the difference in the structure of the ground-state multiplets in holmium gallium borate and aluminum borate. The low magnetic field $B = 0.5$ T and the hyperfine interaction split in a different manner the lowest levels in these two compounds. As a result, as is clearly seen in Fig. 5b, for $HoAl_3(BO_3)_4$, we have a smoothing of the broad peak at 5.5 K, whereas the sharp low-temperature peak arises at a slightly higher temperature than for $HoGa_3(BO_3)_4$. For the latter compound, the behaviors of $C_p/T(T)$ at $B = 0$ and 0.5 T differ only slightly. At $B = 6$ and 9 T, the effects due to the differences in the lower parts of the ground-state multiplets are hardly distinguishable in comparison to the effects produced by the high applied magnetic field. At the same time, the growth of T reveals the effects related to the difference in the population of the levels in the middle part of the multiplet. This is just the cause of the difference in the specific heat values appearing at temperatures approaching 20 K. The measurements at temperatures up to 300 K for $B = 0$ (see inset of Fig. 5b) demonstrate that the types of the behavior of $C_p/T(T)$ for $HoGa_3(BO_3)_4$ and $HoAl_3(BO_3)_4$ are quite similar. However, there exists a significant quantitative difference in the specific heat of these two compounds.

From the above discussion, it is clear that the magnetic properties of $HoGa_3(BO_3)_4$ and $HoAl_3(BO_3)_4$ are rather close to each other. At the same time, they exhibit a substantial difference in the anisotropy of magnetic characteristics and in the contribution of the magnetic subsystem to the specific heat. The latter results from the changes in the CF parameters and hence from the changes in the structure of the ground state multiplet for the Ho^{3+} ion (in the sequence order of singlets and doublets within the set of split levels). Let us discuss how the record magnetoelectric characteristics of $HoAl_3(BO_3)_4$ are affected owing to the replacement of Al^{3+} by Ga^{3+}, to the changes in the CF parameters, and to the magnetic anisotropy.

In Fig. 6, we show the magnetic field dependence of the transverse ($\Delta P_{ba}(B_a)$ and $\Delta P_{bc}(B_c)$) and longitudinal ($\Delta P_{bb}(B_b)$) components of the polarization for $HoGa_3(BO_3)_4$ at different values of T. Here, similarly to the case of $HoAl_3(BO_3)_4$, the growth of the magnetic field is accompanied by the pronounced increase in the anisotropic polarization $\Delta P_b(B_{abc})$. The transverse polarization $\Delta P_{ba}(B_a)$ observed at $T = 5$ K in the magnetic field $B = 9$ T is as high as -1020 μC/m^2. This value far exceeds all known polarization values for iron borates (~300 μC/m^2 in $NdFe_3(BO_3)_4$ [2], ~300 μC/m^2 in $HoFe_3(BO_3)_4$ [26], and ~500 μC/m^2 in $SmFe_3(BO_3)_4$ [27]) and for most aluminum borates (~750 μC/m^2 in $TmAl_3(BO_3)_4$ [10, 12] and ~140 μC/m^2 in $ErAl_3(BO_3)_4$ [12]). Currently, such a value of the polarization is in the second place among those characteristic of $RM_3(BO_3)_4$ borates, being lower only than the record value observed for multiferroics, namely, -5240 μC/m^2 in $HoAl_3(BO_3)_4$ [13].

Thus, we have found that $RM_3(BO_3)_4$ borates with a single magnetic subsystem exhibit the magnetoelectric effect with a large magnitude, which we expected after replacement of the Fe subsystem not only by the aluminum subsystem but also by the gallium one. Here, our interest is attracted not only by the observed high $\Delta P_{ba}(B_a)$ values but also by a rather significant (by a factor of 5) decrease in the polarization in comparison to $HoAl_3(BO_3)_4$. We checked the possible effect of the inversion twinning in the $HoGa_3(BO_3)_4$ single crystal on the obtained result. The X-ray diffraction study of the degree of twinning in $HoGa_3(BO_3)_4$ demonstrates that this crystal completely belongs to the right modification. Note that the similar study of $HoAl_3(BO_3)_4$ single crystals shows that they completely belong to the left modification.

Earlier, several papers reported on the existence of a correlation between the magnetoelectric and magnetoelastic characteristics in $RM_3(BO_3)_4$. For example, $TmAl_3(BO_3)_4$ [10] and $HoAl_3(BO_3)_4$ [11] exhibit a correlation between the magnetic field dependences of polarization and magnetostriction. A similar correlation is found in iron borates [8, 26]. The magnetic field

and temperature dependences calculated in [17] for the multipole moments of Ho^{3+} ion in $HoAl_3(BO_3)_4$ allow the description of the data on magnetostriction reported in [11]. Taking into account the established correlation between the magnetoelectric and magnetoelastic characteristics, we have performed for $HoGa_3(BO_3)_4$ calculations similar to those in [17] and compared the results with the experimental curves for $\Delta P(B)$ (see the magnetoelastic Hamiltonian and the expression for magnetostriction in [17, 28]). According to [17], the largest multipole moments $-\alpha_J\langle O_2^2\rangle$ and $-\beta\langle O_4^2\rangle$ determine the behavior of magnetostriction in $HoAl_3(BO_3)_4$ if the magnetic field lies in the basal plane. In the insets of Figs. 6a and 6b, we show the magnetic field dependence of the actual moment $-\alpha_J\langle O_2^2\rangle$ calculated using CF parameters (7) for **B** || **a**, **b** at the same temperature values as in $\Delta P_b(B_{a,b})$. We see that the characteristic features of the magnetic field and temperature dependences of the moment $-\alpha_J\langle O_2^2\rangle$ are in excellent qualitative agreement with the form of the $\Delta P_b(B_{a,b})$ dependence. This suggests a similar nonlinear form of the magnetostriction $\Delta b/b$ curves, which have not yet been studied experimentally. The magnetic field dependence of the second largest moment $-\beta_J\langle O_4^2\rangle$ exhibits the behavior similar to that of $-\alpha_J\langle O_2^2\rangle$ shown above. Note that the moments $-\alpha_J\langle O_2^2\rangle$ and $-\beta_J\langle O_4^2\rangle$, as well as $\Delta P_b(B_{a,b})$, have opposite signs at **B** || **a** and **B** || **b**. Hence, we should expect that the values of the magnetostriction will have opposite signs for these two field directions. At **B** || **a**, the actual moments undergo larger changes with the field than at **B** || **b**. Therefore, the values of magnetostriction $\Delta b/b$ at **B** || **a** should be larger than those at **B** || **b**. The latter statement correlates well with the ratio of the polarization components at **B** || **a**, **b** and with the result of [11].

In Fig. 7, we show the temperature dependence of the polarization $\Delta P_b(T)$ for $HoGa_3(BO_3)_4$ and $HoAl_3(BO_3)_4$ at the applied magnetic field $B_a = 9$ T, at which the maximum values of ΔP_b are observed. We can see a nonlinear decrease in $\Delta P_b(T)$ resulting from the growing population of the excited states in the ground-state multiplet of the Ho^{3+} ion. One can expect that the different rates of decrease for $\Delta P_b(T)$ are related to the determined differences in the structure of the ground-state multiplets and their different behaviors in a field of 9 T. If we use these dependences to draw the temperature dependence $\Delta P_b^{\mathrm{HoAl-HoGa}}(T) = \Delta P_b^{\mathrm{HoAl}} - \Delta P_b^{\mathrm{HoGa}}$ and compare it with the temperature dependence reflecting the difference of magnetic anisotropies in the same field of 9 T, $\Delta M^{\mathrm{HoGa-HoAl}}(T) = (M_c - M_{\perp c})^{\mathrm{HoGa}} - (M_c - M_{\perp c})^{\mathrm{HoAl}}$ (see Fig. 4), we will

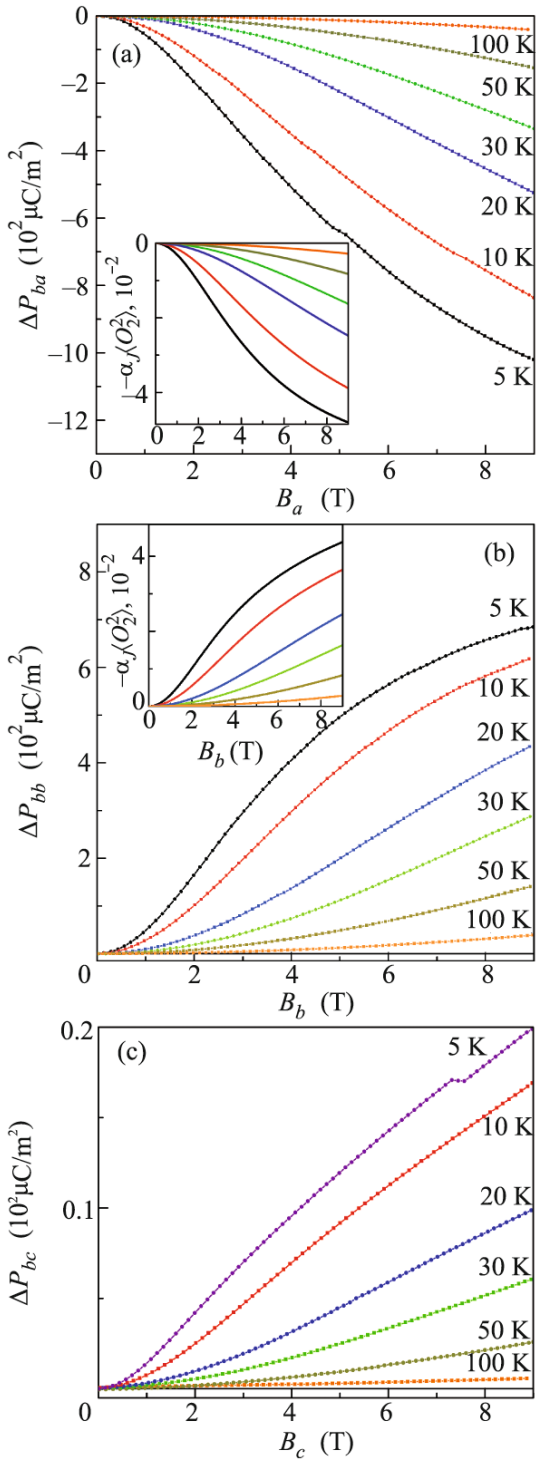

Fig. 6. (Color online) Experimental magnetic field dependence of the (a, c) transverse and (b) longitudinal components of the electric polarization for $HoGa_3(BO_3)_4$ at different values of T indicated near the plots. Insets demonstrate the magnetic field dependence of the multipole moment $-\alpha_J\langle O_2^2\rangle$ of the Ho^{3+} ion at (a) **B** || **a** and (b) **B** || **b** (the curves corresponding to the same temperature values have the same color).

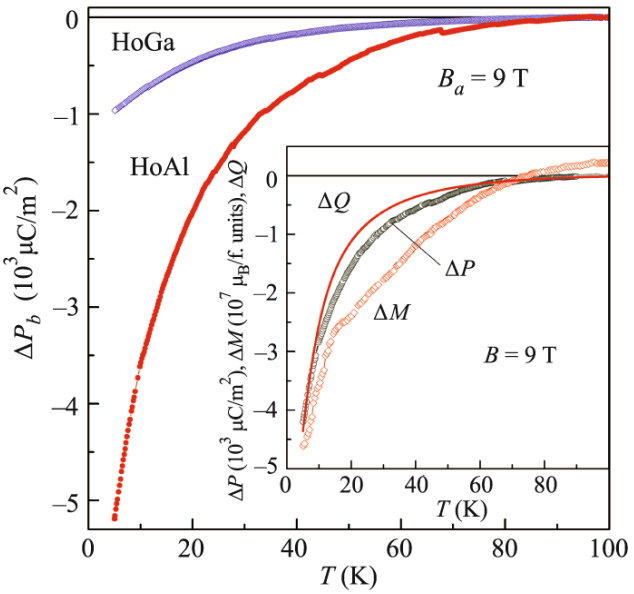

Fig. 7. (Color online) Experimental temperature dependence of the polarization $\Delta P_b(T)$ for (open symbols) $HoGa_3(BO_3)_4$ and (closed symbols) $HoAl_3(BO_3)_4$ at B_a = 9 T. The plots illustrating the temperature dependence of $\Delta P_b^{HoAl-HoGa}(T)$, $\Delta M^{HoGa-HoAl}(T)$, and (red line) $270\Delta Q^{HoAl-HoGa}(T)$ at $B = 9$ T are shown in the inset.

see a good correlation between these curves (see inset of Fig. 7). We can see that the larger the difference in the magnetization anisotropies, the larger $\Delta P_b^{HoAl-HoGa}$. Note that, to draw these plots in the same coordinate system as for $\Delta M^{HoGa-HoAl}(T)$, it is sufficient to use a simple factor of 10^4. In the inset of Fig. 7, we also present the calculated temperature dependence of the difference between the actual moments $-\alpha_J\langle O_2^2\rangle$ for the two compounds: $\Delta Q^{HoAl-HoGa}(T) = -\alpha_J\langle O_2^2\rangle^{HoAl} + \alpha_J\langle O_2^2\rangle^{HoGa}$ at $B_a = 9$ T. It agrees well with the experimental $\Delta P_b^{HoAl-HoGa}(T)$ and $\Delta M^{HoGa-HoAl}$ curves. The good correlation of these temperature dependences allows us to conclude that the pronounced effect on the magnetoelectric characteristics is produced by the changes (due to the replacement of Al^{3+} by Ga^{3+}) in the CF, which forms the electron structure of Ho^{3+} ion (its spectrum and wavefunctions) and is responsible for the anisotropy of magnetic characteristics.

CONCLUSIONS

In summary, we have performed a comprehensive experimental and theoretical study of thermodynamic characteristics of $HoGa_3(BO_3)_4$. It is found that $HoGa_3(BO_3)_4$ exhibits a strong magnetoelectric effect, which is lower only than that in $HoAl_3(BO_3)_4$ among $RM_3(BO_3)_4$. The determined CF parameters allow us to interpret all measured characteristics of $HoGa_3(BO_3)_4$ and their specific features within one approach. We have compared the studied properties of $HoGa_3(BO_3)_4$ with those of $HoAl_3(BO_3)_4$. A good correlation of $\Delta P_b^{HoAl-HoGa}(T)$ with the function $\Delta M^{HoGa-HoAl}(T)$ reflecting the difference in the magnetic anisotropies at $B = 9$ T is found. We conclude that the CF, which forms the electron structure of rare-earth ions and is responsible for the anisotropy of magnetic characteristics, significantly affects the magnetoelectric properties.

The pronounced magnetoelectric effect observed in $HoM_3(BO_3)_4$ (M = Al and Ga) stimulates interest in the further studies of other possible subclasses of $RM_3(BO_3)_4$ borates with a single magnetic subsystem, especially those with holmium ions.

This work was supported by the Russian Foundation for Basic Research (project no. 13-02-12442-ofi_m2). K.N.B. also acknowledges the support from the Council of the President of the Russian Federation for Support of Young Scientists and Leading Scientific Schools (project no. MK-1700.2013.2).

REFERENCES

1. A. K. Zvezdin, S. S. Krotov, A. M. Kadomtseva, G. P. Vorob'ev, A. P. Pyatakov, L. N. Bezmaternykh, and E. A. Popova, JETP Lett. **81**, 272 (2005).
2. A. K. Zvezdin, G. P. Vorob'ev, A. M. Kadomtseva, Yu. F. Popov, A. P. Pyatakov, L. N. Bezmaternykh, A. V. Kuvardin, and E. A. Popova, JETP Lett. **83**, 509 (2006).
3. E. A. Popova, D. V. Volkov, A. N. Vasiliev, A. A. Demidov, N. P. Kolmakova, I. A. Gudim, L. N. Bezmaternykh, N. Tristan, Yu. Skourski, B. Buechner, C. Hess, and R. Klingeler, Phys. Rev. B **75**, 224413 (2007).
4. E. A. Popova, N. I. Leonyuk, M. N. Popova, E. P. Chukalina, K. N. Boldyrev, N. Tristan, R. Klingeler, and B. Buchner, Phys. Rev. B **76**, 054446 (2007).
5. A. A. Mukhin, G. P. Vorob'ev, V. Yu. Ivanov, A. M. Kadomtseva, A. S. Narizhnaya, A. M. Kuz'menko, Yu. F. Popov, L. N. Bezmaternykh, and I. A. Gudim, JETP Lett. **93**, 275 (2011).
6. J. E. Hamann-Borrero, S. Partzsch, S. Valencia, C. Mazzoli, J. Herrero-Martin, R. Feyerherm, E. Dudzik, C. Hess, A. Vasiliev, L. Bezmaternykh, B. Buchner, and J. Geck, Phys. Rev. Lett. **109**, 267202 (2012).
7. A. V. Malakhovskii, A. L. Sukhachev, and A. Yu. Strokova, Phys. Rev. B **88**, 075103 (2013).
8. A. M. Kadomtseva, Yu. F. Popov, G. P. Vorob'ev, A. P. Pyatakov, S. S. Krotov, K. I. Kamilov, V. Yu. Ivanov, A. A. Mukhin, A. K. Zvezdin, A. M. Kuz'menko, L. N. Bezmaternykh, I. A. Gudim, and V. L. Temerov, Low Temp. Phys. **36**, 532 (2010).
9. A. I. Popov, D. I. Plokhov, and A. K. Zvezdin, Phys. Rev. B **87**, 024413 (2013).

10. R. P. Chaudhury, B. Lorenz, Y. Y. Sun, L. N. Bezmaternykh, V. L. Temerov, and C. W. Chu, Phys. Rev. B **81**, 220402 (2010).
11. K.-C. Liang, R. P. Chaudhury, B. Lorenz, Y. Y. Sun, L. N. Bezmaternykh, V. L. Temerov, and C. W. Chu, Phys. Rev. B **83**, 180417(R) (2011).
12. K.-C. Liang, R. P. Chaudhury, B. Lorenz, Y. Y. Sun, L. N. Bezmaternykh, I. A. Gudim, V. L. Temerov, and C. W. Chu, J. Phys.: Conf. Ser. **400**, 032046 (2012).
13. A. I. Begunov, A. A. Demidov, I. A. Gudim, and E. V. Eremin, JETP Lett. **97**, 528 (2013).
14. L. N. Bezmaternykh, V. L. Temerov, I. A. Gudim, and N. A. Stolbovaya, Crystallogr. Rep. **50**, 97 (2005).
15. V. L. Temerov, A. E. Sokolov, A. L. Sukhachev, A. F. Bovina, I. S. Edelman, and A. V. Malakhovskii, Crystallogr. Rep. **53**, 1157 (2008).
16. A. I. Begunov, A. A. Demidov, I. A. Gudim, E. V. Eremin, and D. V. Volkov, in *Proceedings of the 5th Euro-Asian Symposium on Trends in Magnetism: Nanomagnetism (EASTMAG-2013* (Vladivostok, 2013), p. 194.
17. A. I. Begunov, D. V. Volkov, and A. A. Demidov, Phys. Solid State **56**, 511 (2014).
18. A. A. Demidov and D. V. Volkov, Phys. Solid State **53**, 985 (2011).
19. A. A. Demidov, I. A. Gudim, and E. V. Eremin, J. Exp. Theor. Phys. **115**, 815 (2012).
20. A. A. Demidov, I. A. Gudim, and E. V. Eremin, J. Exp. Theor. Phys. **114**, 259 (2012).
21. A. A. Demidov, Z. A. Kazei, N. P. Kolmakova, J.-M. Broto, and H. Racoto, Phys. Rev. B **70**, 134432 (2004).
22. Z. A. Kazei, A. A. Demidov, and N. P. Kolmakova, J. Magn. Magn. Mater. **258–259**, 590 (2003).
23. A. Abragam and B. Bleaney, *Electron Paramagnetic Resonance of Transition Ions* (Clarendon, Oxford, 1970; Mir, Moscow, 1973).
24. A. Baraldi, R. Capelletti, M. Mazzera, N. Magnani, I. Foldvari, and E. Beregi, Phys. Rev. B **76**, 165130 (2007).
25. B. Bleaney, J. F. Gregg, P. Hansen, C. H. A. Huan, M. Lazzouni, M. J. M. Leask, I. D. Morris, and M. R. Wells, Proc. R. Soc. London **416**, 63 (1988).
26. A. M. Kadomtseva, G. P. Vorob'ev, Yu. F. Popov, A. P. Pyatakov, A. A. Mukhin, V. Yu. Ivanov, A. K. Zvezdin, I. A. Gudim, V. L. Temerov, and L. N. Bezmaternykh, J. Exp. Theor. Phys. **114**, 810 (2012).
27. Yu. F. Popov, A. P. Pyatakov, A. M. Kadomtseva, G. P. Vorob'ev, A. K. Zvezdin, A. A. Mukhin, V. Yu. Ivanov, and I. A. Gudim, J. Exp. Theor. Phys. **111**, 199 (2010).
28. A. A. Demidov, N. P. Kolmakova, L. V. Takunov, and D. V. Volkov, Physica B **398**, 78 (2007).

Translated by K. Kugel